14th European Signal Processing Conference (EUSIPCO 2006), Florence, Italy, September 4-8, 2006, copyright by EURASIP

Transport Capacity Regions for Wireless Networks with Multi-User Links

Christian B. Peel, A. Lee Swindlehurst
Brigham Young University
Electrical & Computer Engineering Dept.
459 CB, Provo, UT 84602
chris.peel@ieee.org, swindle@ee.byu.edu

Wolfgang Utschick
Associate Institute for Signal Processing
Munich University of Technology
Arcisstrasse 21, D-80290 Munich, Germany
utschick@tum.de

***Abstract*— We analyze the distance-weighted rate achievable in wireless networks that utilize multiple antennas and multi-user links. We give the transport capacity of multi-antenna multiple-access and broadcast channels, and use these topologies at the physical layer of an ad-hoc network to obtain achievable distance-weighted rate regions for a multi-antenna wireless network. These regions are obtained by utilizing interfering multiple-access and broadcast channel topologies in all possible configurations. A Nash-equilibrium-seeking technique is used to optimize the transmit covariance matrices for each configuration. Multi-hop routing is shown to increase the capacity regions significantly. Numerical examples show the benefit of multiple-access topologies over broadcast and point-to-point links for a uniform per-node power constraint.**

I. Introduction

Wireless networks have been the focus of much recent information theoretical analysis [1]–[3] and protocol and physical layer development [4], [5]. Capacity regions are found in [6] for a single-antenna per node, with point-to-point multi-hop communication. These important results do not use multiple antennas and do not emphasize multi-user coding as a physical-layer technique in wireless networks. We explicitly include multi-antenna multi-user coding in our analysis, and examine distance-weighted rate regions as a function of the power constraint and number of nodes in the network.

The IEEE 802.11 Medium Access Control (MAC) protocol [5] in distributed coordination function (DCF) mode attempts to avoid excessive interference at the receivers in an ad-hoc network, again using point-to-point coding techniques. Analysis of the DCF with large networks [7] indicates that in general the the throughput per node decreases as the density of nodes increases, as in [1]. Despite this work, the best random-access technique for an ad-hoc network has not been found, though specific protocols have been proposed using point-to-point links [4] which offer improvements over simpler MAC protocols. Our work is designed to inform and motivate the use of multi-user links by designers of MAC and physical-layer protocols.

Several researchers have investigated the use of multiple antennas in ad-hoc scenarios. Single-user detection and transmission are considered in [8] and found to give an asymptotic spectral efficiency which scales with M when each node has M antennas. This result assumes that the number of nodes goes to infinity and is independent of the transmit power. The rate regions of [6] are extended for point-to-point MIMO signaling in [9], including average and outage capacity.

In our paper, we give the transport capacity for networks with multiple-antenna multiple-access (MA) and broadcast channel (BC) links, and use these results to give achievable distance-weighted rate regions in an ad-hoc network utilizing these multi-user links. Our results are unique in that they focus on the use of multi-user subnetworks and multiple antennas.

This work was supported by the U. S. Army Research Office under the Multi-University Research Initiative (MURI) grant W911NF-04-1-0224.

II. Background

A. Network Model

Consider a set of K nodes communicating over wireless fading channels using M_k antennas at the kth node. Each node may transmit or receive, but may not do both at the same time. A link is an ordered pair of nodes $[n, m]$ indicating that node n transmits data to node m. A link is active if the transmitting node is radiating a signal designated for the receiving node. Each receiving node collects radiated power from each transmitting node; if any signal is not intended for the receiving node, it is considered to be interference. The level of interference is determined by the fading coefficient between each transmitting and receiving node.

Let $\mathcal{T}$ be the set of all transmitting nodes and let $H_{k,h}$ represent the $M_k \times M_h$ matrix of fading coefficients between nodes h and k; then the received data at node k is

$$\mathbf{y}_k = \sum_{h \in \mathcal{T}} H_{k,h}\mathbf{x}_h + \mathbf{w}_k \quad . \tag{1}$$

Here $\mathbf{x}_h$ is the signal transmitted from node h, and $\mathbf{w}_k$ is the receiver noise observed at node k. Each node has a transmit power constraint P_k. We assume that each node n has full channel state information for all links of the form $[n, m]$ and $[m, n]$ for all m. We assume that $H_{k,h}$ includes the path loss and other attenuation and is typically dependent on $d_{k,h}$, the distance between nodes h and k. For example, in our simulations we assume that the channel between nodes h and k is $H_{k,h} = d_{k,h}^{-\delta}\bar{H}_{k,h}$, where each element of $\bar{H}_{k,h}$ is i.i.d. $\mathcal{CN}(0, 1)$, and δ is the path-loss exponent. We have not yet made a distinction in (1) between nodes in $\mathcal{T}$ which are transmitting to node k and those which are not and nominally act as interference. In the following we specify several link topologies for (1) which distinguish between data-bearing signals and interference. We assume that the channel is static enough that reliable estimates of the coefficients may be obtained, and that these estimates are not so costly as to have a significant impact on the throughput.

B. Link Topologies

There are many different ways that a set of nodes can communicate; they can communicate in a pairwise manner, where each transmitting node designs its signal for only one receiving node. Each receiving node then decodes only the signal intended for it, and treats signals from other transmitting nodes as interference. Most practical techniques and research has focused on this scenario [3]–[8]. This point-to-point coding methodology is illustrated in Figure 1(a), where two links are activated. The task of a MAC protocol is to

control the creation, utilization, and modification of this topology in a distributed manner. For example, slotted ALOHA allows a node to transmit whenever it has data to send, resulting in a collision when the intended receiver is transmitting, or is subject to more interference than it can reject.

Though there has been much work on MAC protocols for ad-hoc networks, it is not yet clear what rate a throughput-optimal medium access protocol might achieve. One approach is to utilize a full search over all topologies; though not necessarily practical, this technique gives results which are useful as a benchmark. In Sections IV and V we use this approach to show that certain topologies are better in terms of distance-weighted throughput than others. As we will show, for per-node power constraints, networks connected utilizing MA links as in Figure 1(b) perform better than networks connected with point-to-point or BC links.

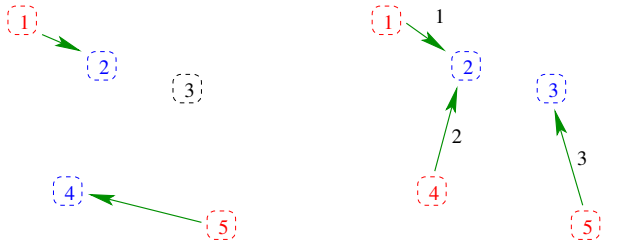

(a) Network with Point–to–Point links (b) Network with MA link

Fig. 1. Network link topology when (a) only point-to-point communications links are possible, and (b) when MA communications links are possible.

We partition the set of nodes $\{1,\ldots,K\}$ into L non-intersecting subsets, or sub-networks, with N_l nodes in the lth sub-network $\mathbf{z}_l$. Nodes within a sub-network cooperate to exchange data. Nodes in different sub-networks are assumed to be able to exchange information when they are joined in a sub-network at a later time instant, or by the aid of a higher-layer routing protocol. Denoting the partition as Z, we write

$$Z = \{\mathbf{z}_1,\ldots,\mathbf{z}_L\} \ . \tag{2}$$

A *transmission scheme* controls the way that a sub-network is configured. For example, in a point-to-point scheme each sub-network consists of a single transmitter and a single receiver. We also consider broadcast channel and multiple-access schemes. Other possible sub-network topologies that we do not have space to consider include the relay channel [2] and multiple node strategies such as cooperative diversity [10].

III. Sub-networks and Schedules

A. Sub-Network Capacity

We consider several ways that a single sub-network $\mathbf{z}$ may be configured for information transfer. Figure 1(a) shows two pairs of nodes communicating using point-to-point links, where each receive node only knows about the corresponding transmit node, and treats other received signals as noise. The capacity-achieving transmission technique for a point-to-point network with complete channel state information (CSI) at both terminals [11] utilizes a waterfilling solution to find the power to allocate to each eigenmode of the channel; in the following we express this in the transmit covariance matrix S. For a transmit-receive pair $[a,b]$, the received data is

$$\mathbf{y}_b = H_{a,b}\mathbf{x}_a + \mathbf{w}_b \ . \tag{3}$$

The achievable rate is then

$$C(\mathbf{z}) = \max_{\mathrm{tr}(S)\le P_a} \log_2 \frac{|S_{\mathbf{w}_b} + H_{a,b}(\mathbf{z})SH^*_{a,b}(\mathbf{z})|}{|S_{\mathbf{w}_b}|} \ , \tag{4}$$

where $S_{\mathbf{w}_b}$ is the noise covariance. This can be solved via waterfilling to satisfy the power constraint P_a. In our wireless network, we are interested not only in rate, but in the distance that bits are transmitted. Gupta and Kumar defined transport capacity [1] as the distance-weighted rate, maximized over the topology and signaling scheme. The transport capacity for a point-to-point sub-network $\mathbf{z}$ with full CSI is

$$T^{P2P}(\mathbf{z}) = d_{a,b}(\mathbf{z})C(\mathbf{z}) \ . \tag{5}$$

We state this equation as a function of the subnetwork $\mathbf{z}$ to emphasize that the distances $d_{a,b}$ and capacity are dependent on the sub-network topology. For the rest of this section we will not explicitly show this dependence.

The second configuration of a sub-network that we consider is in a MA topology in which many users communicate with a single access point. We will use this topology later on to characterize a network that is communicating at the physical layer using several distinct multiple-access links, as shown in Figure 1(b). Consider the case where node b is receiving data from nodes $a_l, l = 1,\ldots,K_u$. The system model is thus

$$\mathbf{y}_b = \sum_{l=1}^{K_u} H_{a_l,b}\mathbf{x}_{a_l} + \mathbf{w}_b \ , \tag{6}$$

where $\mathbf{w}_b$ includes both receiver noise and interference from other transmitting nodes, and has covariance matrix $S_{\mathbf{w}_b}$. The rates achievable for transmit covariance matrices S_{a_l} are [12]

$$R_{a_{\pi(l)}} = \log_2 \frac{|S_{\mathbf{w}_b} + \sum_{k=l}^{K_u} H_{a_{\pi(k)},b}S_{a_{\pi(k)}}H^*_{a_{\pi(k)},b}|}{|S_{\mathbf{w}_b}|} - \sum_{k=l+1}^{K_u} R_{a_{\pi(k)}} \ , \tag{7}$$

for $l = 1,\ldots,K_u$, where π represents the decoding order (user $\pi(1)$ is decoded first). The boundary of the capacity region is found by maximizing

$$\mu_1 R_{a_1} + \ldots + \mu_{K_u} R_{a_{K_u}} \tag{8}$$

over S_{a_l}, $l = 1,\ldots,K_u$ which satisfy $\mathrm{tr}(S_{a_l}) \le P_{a_l}$, and where the non-negative weights satisfy $\sum_k \mu_k = 1$. Each set of covariance matrices thus found gives a point on the capacity region boundary. In our simulations, we use an approximation to the rate region boundary obtained after one iteration of the sum-capacity-achieving technique of [12]. Simulations and analysis show that this approximation is quite good.

Lemma 1: Let π be a permutation such that $d_{a_{\pi(1)},b} \le d_{a_{\pi(2)},b} \le \ldots \le d_{a_{\pi(K_u)},b}$. The transport capacity of the MA channel (6) is found by decoding users in the order $\pi(1),\ldots,\pi(K_d)$, with the exact value given by:

$$T^{MA} = \max_{\mathrm{tr}(S_{a_{\pi(k)}})\le P_{a_{\pi(k)}}} \sum_k d_{a_{\pi(k)},b}R_{a_{\pi(k)}}(S_{a_{\pi(1)}},\ldots,S_{a_{\pi(K_u)}}) \ . \tag{9}$$

Proof: By letting $\mu_k = d_{a_k,b}/\sum_j d_{a_j,b}$ in (8) we can find the transmit covariance matrices and rates which achieve the sum transport capacity, then use (9) to obtain the exact value. An argument similar to that in [13] for the scalar MA channel gives the decoding order. ■

The multi-antenna BC has received considerable attention recently [14], [15]. Consider the case where node a transmits to nodes $b_l, l = 1, \ldots, K_d$, then the system model is:

$$\mathbf{y}_{b_l} = H_{a,b_l}\mathbf{x}_a + \mathbf{w}_{b_l} \ , \ \ l = 1, \ldots, K_d \ , \tag{10}$$

where $\mathbf{w}_{b_l}$ includes interference from other transmitting nodes and receiver noise, and has covariance matrix $S_{\mathbf{w}_{b_l}}$. The rates achievable for a fixed set of covariance matrices S_{b_l}, $l = 1, \ldots, K_d$ for the downlink satisfy [15], [16]

$$R_{b_{\pi(n)}} \leq \log_2 \frac{|\sum_{k=n}^{K_d} H_{a,b_{\pi(n)}} S_{b_{\pi(k)}} H^*_{a,b_{\pi(n)}} + S_{\mathbf{w}_{b_{\pi(n)}}}|}{|\sum_{k=n+1}^{K_d} H_{a,b_{\pi(n)}} S_{b_{\pi(k)}} H^*_{a,b_{\pi(n)}} + S_{\mathbf{w}_{b_{\pi(n)}}}|} \ , \tag{11}$$

where the S_{b_k} satisfy the sum power constraint $\sum_{k=1}^{K_d} \mathrm{tr}(S_{b_k}) \leq P_a$, and π is the decoding order.

The boundary of the rate region is characterized by the set of rate vectors which solve the following optimization problem

$$\max_{S_{b_k}: \ \mathrm{tr}(S_{b_k}) \leq P_a} \sum_{k=1}^{K_d} \mu_k R_{b_k}(S_{b_1}, \ldots, S_{b_{K_d}}) \ , \tag{12}$$

for weight vectors such that $\sum_{k=1}^{K_d} \mu_k = 1$. Because the rate region for a set of covariance matrices is a polymatroid, the best decoding order is that where $\mu_{\pi(1)} \geq \mu_{\pi(2)} \geq \ldots \geq \mu_{\pi(K_u)}$. An efficient algorithm for solving this convex optimization problem is presented in [17]. This algorithm solves for transmit covariance matrices for the dual MA channel, which can then be converted to BC covariance matrices using the method of [14].

Lemma 2: Let π be a permutation such that $d_{a_{\pi(1)},b} \geq d_{a_{\pi(2)},b} \geq \ldots \geq d_{a_{\pi(K_u)},b}$. The transport capacity of the broadcast channel (10) is

$$T^{BC} = \max_{\mathrm{tr}(S_{b_{\pi(k)}}) \leq P_a} \sum_k d_{a,b_{\pi(k)}} R_{b_{\pi(k)}}(S_{b_1}, \ldots, S_{b_{K_d}}) \ . \tag{13}$$

Proof: By letting $\mu_k = d_{a,b_k} / \sum_j d_{a,b_j}$ in (12) we can find the transmit covariance matrices and rates that achieve the sum transport capacity, and then use (13) to obtain the exact value. ■

IV. Single-Hop Routing and Sum Capacity

For a network of K nodes, the Bell number B_K gives the number of ways the network can be separated into sub-networks:

$$B(K) = \left\lceil \frac{1}{e} \sum_{m=1}^{2K} \frac{m^K}{m!} \right\rceil \ . \tag{14}$$

Let $\{b^i_1, \ldots, b^i_{L_i}\}$ denote the sizes of sub-networks in the ith Bell partition (we assume that nodes in sub-networks of size one are silent, and that the corresponding $b^i_j = 0$), where L_i is the number of active sub-networks in the ith partition. There are N ways to arrange a sub-network of size N into an MA network; for every Bell partition there are $\prod_{j=1}^{L_i} b^i_j$ possible MA partitions. The number of possible schedules for a network of K nodes using only MA coding is

$$N^{MA}(K) = 1 + \sum_{i=1}^{B(K)} \prod_{j=1}^{L_i} b^i_j \ , \tag{15}$$

where the "1" term is added to include the possibility of no nodes being active. We note that this is also the number of possible ways to configure a network into BC sub-networks, without using MA coding: $N^{BC}(K) = N^{MA}(K)$. A similar technique can be used to find the number of point-to-point schedules possible [6], which we label N^{P2P}_K.

Table I lists values of $B(K)$, $N^{P2P}(K)$, and $N^{MA}(K)$ for $K = 1, \ldots, 10$, as found by enumerating all Bell partitions, finding the corresponding values of b^i_j and calculating $N^{MA}(K)$ using (15). Though a network of size $K = 10$ is not exceptionally large, there are over two million ways that it can be separated into MA or BC networks.

K	$B(K)$	$N^{P2P}(K)$	$N^{MA}(K)$
1	1	1	1
2	2	3	3
3	5	7	10
4	15	25	41
5	52	81	196
6	203	331	1057
7	877	1303	6322
8	4140	5379	41393
9	21147	26785	293608
10	115975	133651	2237921

TABLE I

Number of possible schedules using point-to-point and MA networks. Bell's number is included for reference.

Let $\mathcal{Z}^{P2P}$, $\mathcal{Z}^{BC}$, and $\mathcal{Z}^{MA}$ be sets of all possible point-to-point, BC, and MA schedules, respectively. The network transport capacity when considering all possible MA, BC and point-to-point topologies is given by the following equations:

$$\mathcal{T}^{P2P}_{SH} = \max_{Z_j \in \mathcal{Z}^{P2P}} \sum_{\mathbf{z} \in Z_j} T^{P2P}(\mathbf{z}) \ , \tag{16}$$

$$\mathcal{T}^{BC}_{SH} = \max_{Z_j \in \mathcal{Z}^{BC}} \sum_{\mathbf{z} \in Z_j} T^{BC}(\mathbf{z}) \ , \tag{17}$$

$$\mathcal{T}^{MA}_{SH} = \max_{Z_j \in \mathcal{Z}^{MA}} \sum_{\mathbf{z} \in Z_j} T^{MA}(\mathbf{z}) \ . \tag{18}$$

Interference between sub-networks is included in these bounds through noise covariance matrices, which is not shown explicitly for brevity of exposition. We use a distributed algorithm to successively optimize the covariance matrices for each sub-network, while maintaining the transmit covariance matrices for other sub-networks constant. Considering the covariance optimization problem as a non-cooperative game between the sub-networks, our method seeks a Nash equilibrium, or the set of covariance matrices such that the distance-weighted rate for a sub-network would decrease by changing only its own covariance matrices. The distributed nature of this algorithm could be implemented in a similar way to (e.g.) the progressive ramp up algorithm (PRUA) for power control in ad-hoc networks [4]. Simulations show that our method typically converges to a Nash equilibrium (for all types of sub-network) in one or two full iterations over the network. The covariance matrices were initialized to be scaled identities, before optimization. A similar algorithm was presented in [18] for point-to-point multi-antenna networks.

Figure 2 shows (16), (17), and (18) as a function of the power constraint P_k for a system with $K = 5$ nodes and $M = 4$ antennas per node. Two full iterations of the Nash-equilibrium-seeking covariance optimization algorithm were used, with results included regardless of whether or not convergence occurred. The MA bound is higher at all power levels, but has a more significant advantage at high power. Though the BC bound is better than the point-to-point bounds, the advantage is not as dramatic as for the MA case.

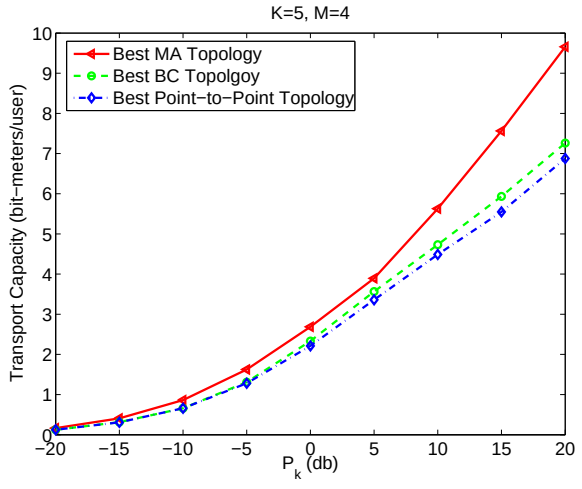

Fig. 2. The bounds (16), (17), and (18) on the transport capacity of a network as a function of the power constraint P_k for a system with $K = 5$ nodes and $M = 4$ antennas. The MA bound gives higher throughput than use of point-to-point or BC constraints.

V. Multi-Hop Routing and Capacity Regions

We now turn to multi-hop routing, utilizing the multi-user transmission schemes presented above. Modern transmission schemes move packets along a path involving several nodes, which obviates the requirement that each node communicate directly to every other node in the network. Because of the flexibility induced, multi-hop routing increases the range of rates at which data can be transferred. Our work is novel in that we allow multi-user links, in contrast to the point-to-point links of [6], [9]. For simplicity, we do not allow successive interference cancellation, power control, or transmission at a restricted set of rates; we expect these techniques to be beneficial similar to the case of single-antenna terminals [6].

To enable mathematical manipulation, we represent the distance-weighted rates achievable on various links in a transmission scheme with rate matrices [6]. For a network with K nodes, a $K \times K$ rate matrix T has as elements

$$t_{ij} = \begin{cases} d_{ij}r, & \text{if node with index } j \text{ receives information at rate } r \text{ with node } i \text{ as the original source,} \\ -d_{ij}r, & \text{if node } j \text{ transmits information at rate } r \text{ with node } i \text{ as the original source,} \\ 0, & \text{otherwise,} \end{cases} \tag{19}$$

where d_{ij} is the distance between nodes i and j. Figure 1(b) shows rates next to the links in a MA sub-network. The rate matrix for this network assuming single-hop routing and $d_{1,2} = d_{4,2} = d_{5,3} = 1$ is

$$T_1 = \begin{bmatrix} -1 & 1 & 0 & 0 & 0 \\ 0 & 0 & 0 & 0 & 0 \\ 0 & 0 & 0 & 0 & 0 \\ 0 & 2 & 0 & -2 & 0 \\ 0 & 0 & 3 & 0 & -3 \end{bmatrix} . \tag{20}$$

Another rate matrix is to assume that all the the data (in the same figure) originates at node 5, in which case the rate matrix is

$$T_2 = \begin{bmatrix} 0 & 0 & 0 & 0 & 0 \\ 0 & 0 & 0 & 0 & 0 \\ 0 & 0 & 0 & 0 & 0 \\ 0 & 0 & 0 & 0 & 0 \\ -1 & 3 & 3 & -2 & -3 \end{bmatrix} . \tag{21}$$

For each transmission scheme, a finite set of rate matrices are possible; the previous section enumerates the single-hop possibilities; the rate matrices for each are readily found using the power constraints P_k, the channels $H_{j,k}$ and (e.g.) (5). In contrast, we are interested in multi-hop communication; in this case the number of possible rate matrices is increased significantly, since the data transferred on each link may originate at any of the K nodes in the network. This readily leads to an equation for the number of multi-hop rate matrices in a network of size K

$$N_{MH}^{MA}(K) = 1 + \sum_{i=1}^{B(K)} \prod_{j=1}^{L_i} b_j^i K^{b_j^i - 1} , \tag{22}$$

which is also the number of BC matrices ($N_{MH}^{BC}(K) = N_{MH}^{MA}(K)$). The number of point-to-point multi-hop matrices $N_{MH}^{P2P}(K)$is similarly defined [6].

Given a set of N_M distance-weighted rate matrices $\{T_1, \ldots, T_{N_M}\}$ the transport capacity region is

$$\mathcal{T} = Co(\{T_i\}) \cap \mathcal{P}_n , \tag{23}$$

where $\mathcal{P}_n$ is the set of all $K \times K$ matrices with zeros along the diagonal and nonnegative elements off the diagonal, and $Co(\{T_i\})$ indicates the convex hull of the set of matrices $\{T_i\}$. Capacity matrices for multi-hop networks utilizing point-to-point, BC, and MA links can be calculated using equations (5), (9), and (13), respectively. The corresponding multi-hop capacity regions are

$$\mathcal{T}_{MH}^{P2P} = \left\{ \sum_{i=1}^{N_{MH}^{P2P}(K)} \alpha_i T_i^{P2P} : \sum_{i=1}^{N_{MH}^{P2P}(K)} \alpha_i \leq 1 \right\} \cap \mathcal{P}_n \tag{24}$$

$$\mathcal{T}_{MH}^{BC} = \left\{ \sum_{i=1}^{N_{MH}^{BC}(K)} \alpha_i T_i^{BC} : \sum_{i=1}^{N_{MH}^{BC}(K)} \alpha_i \leq 1 \right\} \cap \mathcal{P}_n \tag{25}$$

$$\mathcal{T}_{MH}^{MA} = \left\{ \sum_{i=1}^{N_{MH}^{MA}(K)} \alpha_i T_i^{MA} : \sum_{i=1}^{N_{MH}^{MA}(K)} \alpha_i \leq 1 \right\} \cap \mathcal{P}_n , \tag{26}$$

where in all cases the coefficients α_i satisfy $\alpha_i \geq 0$. Single-hop capacity regions for networks utilizing point-to-point, BC, and MA links may be similarly defined.

This convex combination of basic rate matrices defines a rate for each of K nodes talking with the remaining $K - 1$ nodes, and a $K(K-1)$-dimensional rate region results. We note that the routing scheme defined by (23) is not necessarily causal; packets may be transmitted from a relay node before they arrive. A start-up period in which a large backlog of packets is distributed around the network takes care of this problem, as has been noted in [6].

As an example, consider the three-node network consisting of only nodes 1, 2, and 4 in the MA configuration shown in Figure 1(b). Using the techniques described in Section IV for a given set of channel coefficients, power constraints, and node locations, a rate matrix for this configuration can be specified. This rate matrix will characterize the point on the capacity region boundary for this multiple-access channel which gives the highest distance-weighted sum rate; a rate matrix such as in (20) can easily be written to characterize these rates. We note, however, that other points contained in the capacity region of the MA channel may be of interest. For example in a larger network the transmit nodes may be forwarding data for other nodes, in which case the rate should be weighted by the end-to-end distance, rather than the distance the bits travel along the link. We do not pursue this possibility further in the present work,

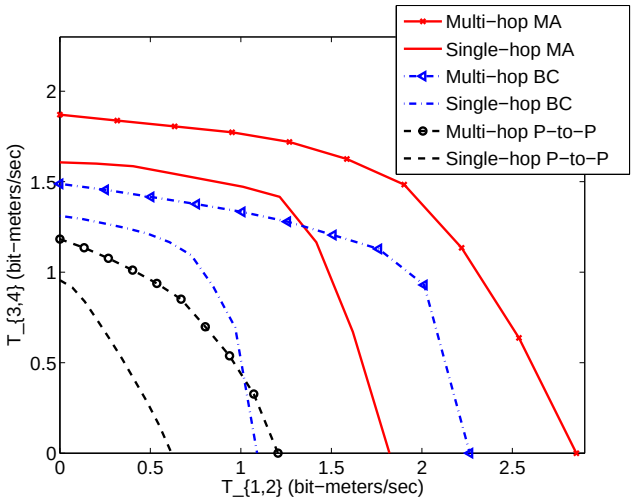

Fig. 3. This figure shows transport rate regions for rates $T_{1,2}$ versus $T_{3,4}$ for a six-node network where underlying links are allowed to be configured as point-to-point channels, BC, and MA channels. The multi-hop regions are calculated using (24), (25), (26), respectively. Transmission schemes that allow multi-user links and multi-hop routing give higher performance than network topologies that use point-to-point links and single-hop routing.

but note that sampling the capacity region of sub-networks to better approximate the full capacity region leads to an exponential increase in the number of rate matrices with the number of nodes in a network (beyond the already-factorial growth shown in Table I).

Figure 3 shows transport rate regions for several transmission schemes. The simulation shows results for a single five-node network, with node locations chosen independently from a zero-mean circularly-symmetric Gaussian distribution with variance $1/\sqrt{2}$ in each direction. The channel coefficients are also chosen from an i.i.d. distribution as described in Section II-A with path-loss exponent $\delta = 2$. All end-to-end rates besides the rates of interest ($T_{1,2}$ and $T_{3,4}$) are constrained to be 0.4 bit-meters/sec, regardless of the routing or type of links allowed. In the figure, the transmission scheme which allows multi-hop communication and MA links has a significantly higher throughput than the other methods.

Though capacity regions characterize all achievable rates, other metrics are also useful. The sum capacity defined in Section IV is one important measure. It is straightforward to show using the convexity of the multi-hop capacity region definition (23), that the sum capacity for single-hop and multi-hop routing are the same. Another useful tool is the *uniform capacity* [6] which is the maximum distance-weighted rate t in a multi-hop network such that every end-to-end link achieves transport rate t. Simulations show that this metric has much the same behavior as the sum capacity of Section IV.

VI. Discussion

Important topics for further study include the best way to acquire the channel state, the benefit of transmit CSI over receive-only CSI, and whether CSI for adjacent nodes is required in addition to CSI for channels impinging on a node. It is apparent that methods are needed for obtaining the best network topology that are of lower complexity than a full search over all possible network combinations. Preliminary investigation shows that polynomial algorithms (in the number of nodes) can approach the performance of full-search techniques. It is also not obvious whether a simple MAC protocol such as Aloha or CSMA/CA is sufficient or if other new protocols are prescribed.

The distributed algorithm for covariance optimization that we present (which seeks a Nash equilibrium) could be improved using for example a gradient projection optimization [18]. Though such a technique would give results useful for comparison and analysis, the global CSI required does not engender the distributed approach required for practical algorithms. In future ad-hoc networks, nodes will obtain packets from neighboring nodes, then cooperate to retransmit and forward them on. Bounds similar to those for the BC and MA cases developed above could be constructed using cooperative transmission topologies [2], [10].

References

[1] P. Gupta and P. Kumar, "The capacity of wireless networks," *IEEE Transactions on Information Theory*, vol. 46, no. 2, pp. 388–404, March 2000.

[2] G. Kramer, M. Gastpar, and P. Gupta, "Capacity theorems for wireless relay channels," in *Proc. 41st Annual Allerton Conf. on Commun., Control and Comp.*, Monticello, IL, USA, October 2003, pp. 1074–1083.

[3] F. Xue, L.-L. Xie, and P. Kumar, "The transport capacity of wireless networks over fading channels," *IEEE Transactions on Information Theory*, vol. 51, no. 3, pp. 834–847, March 2005.

[4] S. Toumpis and A. Goldsmith, "Performance, optimization, and cross-layer design of media access protocols for wireless ad hoc networks," in *Proc. IEEE International Conference on Communications*, vol. 3, Anchorage, AK, USA, May 2003, pp. 2234–2240.

[5] "IEEE Std 802.11-1997 Wireless LAN Medium Access Control And Physical Layer Specifications," pp. i–445, November 1997.

[6] S. Toumpis and A. Goldsmith, "Capacity regions for wireless ad hoc networks," *Wireless Communications, IEEE Transactions on*, vol. 2, no. 4, pp. 736–748, July 2003.

[7] J. Li, C. Blake, D. S. D. Couto, H. I. Lee, and R. Morris, "Capacity of ad hoc wireless networks," in *MobiCom '01: Proceedings of the 7th annual international conference on Mobile computing and networking*. New York, NY, USA: ACM Press, 2001, pp. 61–69.

[8] B. Chen and M. J. Gans, "Limiting throughput of MIMO ad hoc networks," in *Proceedings IEEE International Conference on Acoustics, Speech, and Signal Processing*, vol. 3, March 2005, pp. 393–396.

[9] S. Ye and R. S. Blum, "On the rate regions for wireless MIMO ad hoc networks," in *Proc. Vehicular Technology Conference (VTC)*, Los Angeles, Sept. 2004, pp. 1648–1652.

[10] J. Laneman and G. Wornell, "Distributed space-time-coded protocols for exploiting cooperative diversity in wireless networks," *IEEE Transactions on Information Theory*, vol. 49, no. 10, pp. 2415–2425, October 2003.

[11] I. E. Telatar, "Capacity of multi-antenna Gaussian channels," *European Trans. Telecommunications*, vol. 10, no. 6, pp. 585–595, Nov/Dec 1999.

[12] W. Yu, W. Rhee, S. Boyd, and J. M. Cioffi, "Iterative water-filling for Gaussian vector multiple-access channels," *IEEE Transactions on Information Theory*, vol. 50, no. 1, pp. 145–152, January 2004.

[13] G. Gupta, S. Toumpis, J. Sayir, and R. R. Müller, "On the transport capacity of Gaussian multiple access and broadcast channels," in *Proc. IEEE ISIT*, Adelaide, Australia, September 2005.

[14] S. Vishwanath, N. Jindal, and A. Goldsmith, "Duality, achievable rates and sum capacity of Gaussian MIMO broadcast channels," *IEEE Transactions on Information Theory*, vol. 49, no. 10, pp. 2658–2668, August 2003.

[15] H. Weingarten, Y. Steinberg, and S. Shamai, "The capacity region of the Gaussian MIMO broadcast channel," in *Proceedings Conf. on Information Sciences and Systems (CISS)*, Princeton, NJ, March 2004.

[16] P. Viswanath and D. Tse, "Sum capacity of the vector Gaussian broadcast channel and uplink-downlink duality," *IEEE Transactions on Information Theory*, vol. 49, no. 8, pp. 1912–1921, August 2003.

[17] H. Viswanathan, S. Venkatesan, and H. Huang, "Downlink capacity evaluation of cellular networks with known-interference cancellation," *IEEE Journal on Selected Areas in Communications*, vol. 21, no. 5, pp. 802–811, June 2003.

[18] S. Ye and R. S. Blum, "Optimized signaling for MIMO interference systems with feedback," *IEEE Transactions on Signal Processing*, vol. 51, no. 11, pp. 2839–2848, Nov. 2003.